JOURNAL OF MATERIALS SCIENCE **36** (2001) 2435–2440

An amorphous ceramic $Al_{32.4}Er_{7.6}O_{60}$ fiber with large viscous flow deformation and a high-strength nanocrystallized ceramic fiber

Y. WAKU
Japan Ultra-high Temperature Materials Research Institute, Ube City, Yamaguchi, 755-0001, Japan
E-mail: waku@jutem.co.jp

H. OHTSUBO
Ube Research Laboratory, Corporate & Development, UBE Industries, Ltd., Ube City, Yamaguchi,755-8633, Japan

T. TAKAHASHI
Japan Ultra-high Temperature Materials Research Institute, Ube City, Yamaguchi, 755-0001, Japan

A. INOUE
Institute for Materials Research, Tohoku University, Sendai, 980-8577, Japan

An amorphous ceramic $Al_{32.4}Er_{7.6}O_{60}$ continuous fiber with a diameter of about 20 μm could be made successfully by using the melt extraction method. This fiber shows large viscous flow deformation at the supercooled liquid state (about 1273 K). The fiber's tensile strength is about 900 MPa and this strength is maintained up to around 1100 K. A high-strength continuous ceramic fiber with a uniform $Er_3Al_5O_{12}$ nanocrystalline phase in an amorphous matrix can also be obtained with suitable crystallization from the amorphous state by heat treatment. The heat resistance, Young's modulus, and other properties are therefore improved. The nanocrystallized fiber which was heat-treated at 1373 K for 2 hours in an air atmosphere has a maximum room temperature tensile strength of 1.9 GPa, around twice that of an as-extracted amorphous fiber. The amorphous continuous ceramic fiber is promising as a ceramic that can be easily shaped at relatively low temperatures (about 1273 K), and as a reinforcing fiber for composites that can undergo secondary processing. Furthermore, this fiber can be considered as more superior to glass fibers because of its greater high-temperature strength and its high Young's modulus.

1. Introduction

Continuous ceramic fibers are being actively researched worldwide as potential reinforcing fibers for monolithic ceramics and metallic materials [1–4]. One of the huge impediments to their practical application is that, because composites reinforced with such fibers can not undergo secondary processing, the strengthening of complex shapes is difficult. If a ceramic continuous fiber that could undergo secondary processing were developed, the composite could be formed into complex shapes.

Amorphous and mixed crystal phase ceramic fibers have been obtained using the melt extraction method in the ZrO_2-Al_2O_3 systems and the CaO-Al_2O_3 systems [5, 6]. Amorphous alumina fibers have also been obtained using the inviscid melt spinning method in the CaO-Al_2O_3 systems [7, 8]. Characterization of an amorphous Y_2O_3-Al_2O_3 fiber made using the melt extraction method has recently been reported [9]. But this fiber displayed neither the viscous flow deformation nor the existence of a supercooled liquid state on a differential thermal analysis (DTA) curve [9]. In relation to this, Waku *et al*. have recently reported on an amorphous $Al_{31}Gd_9O_{60}$ ceramic fiber with large viscous flow deformation in a supercooled state [10].

We have now attempted to fabricate a ceramic continuous fiber with an Al_2O_3/Er_2O_3 eutectic composition using the melt extraction method. The first objective of this study was to obtain an amorphous continuous ceramic fiber, with similar viscous flow properties to the $Al_{31}Gd_9O_{60}$ fiber. The second objective is to obtain a high-strength continuous ceramic fiber with a uniform nanocrystalline phase in an amorphous matrix by utilizing the crystallization from an amorphous state by heat treatment.

2. Experimental procedure

2.1. Manufacturing of raw powders

Commercially available Al_2O_3 powder (AKP-30 made by Sumitomo Chemical Co., Ltd., Tokyo, Japan) and Er_2O_3 powder (Er_2O_3-RU made by Shin-etsu Chemical Co., Ltd., Tokyo, Japan) were mixed to a mole ratio of $Al_2O_3/Er_2O_3 = 81/19$, and wet ball-milled using ethanol, to obtain a homogeneous powder. The slurry obtained was dried in a rotary evaporator to remove the ethanol. After pre-forming the mixed powder into a pellet 10 mm in diameter and 10 mm in height, it was premelted in an arc discharge.

2.2. Melt extraction method

The resultant ingot was arc-melted again and the melt was brought into contact with copper rollers (diameter: 70 mm; thickness: 0.5 mm) that had V-shaped edges (30°) and were rotating at a peripheral speed of 2 m/sec, producing a fiber with an approximate diameter of 20 μm. Fabrication of the melt and fiber was conducted in an argon gas atmosphere of 300–500 mm Hg.

2.3. Evaluation method

The tensile specimen was a fiber with a total length of 45 mm and span of 25 mm at room temperature and a total length of 120 mm and span of 100 mm at high temperatures. The tensile tests were conducted from room temperature to 1573 K at a crosshead speed of 2 mm/min in an air atmosphere after maintaining for 8 minutes at the test temperatures. The equipment used was a TENSILON/UTM-II-20 (made by Orientec Corporation, Tokyo, Japan).

Differential thermal analysis (DTA) was performed at a heating rate of 40 K/min, using a TG/DTA320 (made by Seiko Instruments, Chiba, Japan). A Rigaku-Denki RAD-RB type X-ray diffraction apparatus was used for structural analysis and the fiber structure was observed using a Japan Electron JEM-2010 electron microscope.

3. Results and discussion

3.1. Characterization of ceramic fibers

SEM images of the fiber directional shape of the $Al_{32.4}Er_{7.6}O_{60}$ fiber obtained with the melt extraction method are shown in Fig. 1. An X-ray diffraction pattern of the fiber is shown in Fig. 2. It is evident that the fiber is a continuous fiber with a diameter of about 20 μm and a relatively smooth surface (Fig. 1). The transverse cross sectional shape of a fabricated fiber is nearly close to a perfect circle. The X-ray diffraction pattern shows broad peaks with the largest intensity at a wave vector ($K_p = 4\pi \sin\theta/\lambda$) of 21.7 nm^{-1}. This result indicates that the fiber has an amorphous structure, in agreement with the results of the bright-field electron image and selected-area electron diffraction pattern consisting only of halo rings.

The DTA of this fiber is shown in Fig. 3. The glass transition temperature (T_g) is close to about 1173 K, and that an endothermic reaction occurs afterward, indicating the existence of a supercooled liquid state at about 1173 K–1225 K (= Tx1 − Tg, Tx1 is the onset temperature defined as the intersection point of the tangential lines on the DTA curves between supercooled liquid and exothermic peak increases from 1225 K). Both Tg

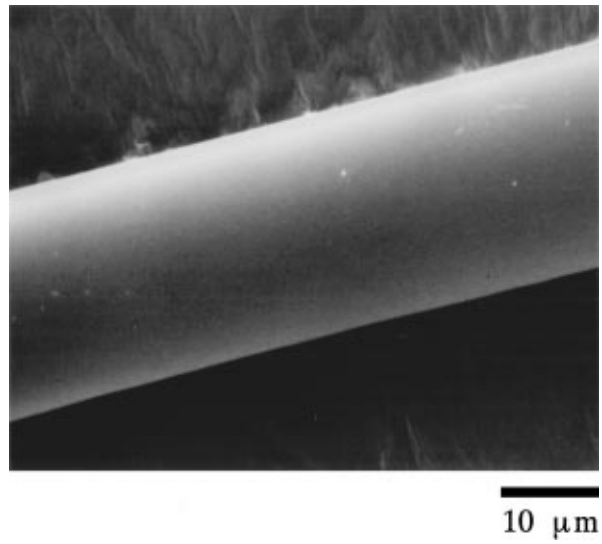

Figure 1 SEM image showing the external appearance in the fiber direction of an $Al_{32.4}$ $Er_{7.6}O_{60}$ continuous fiber made with melt extraction method.

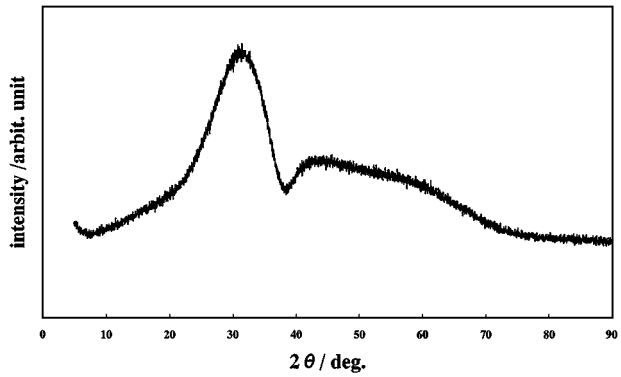

Figure 2 An x-ray diffraction pattern of an $Al_{32.4}Er_{7.6}O_{60}$ continuous fiber made with melt extraction method.

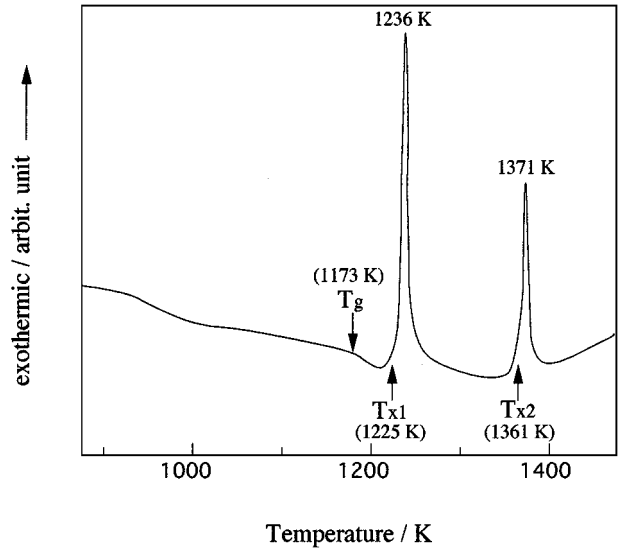

Figure 3 A differential thermal analysis (DTA) curve of an amorphous $Al_{32.4}Er_{7.6}O_{60}$ continuous fiber made with melt extraction method.

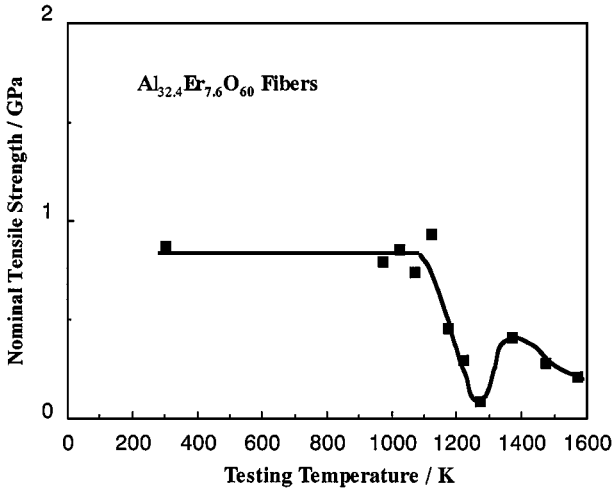

Figure 4 Temperature dependence of tensile strength of an amorphous $Al_{32.4}Er_{7.6}O_{60}$ continuous fiber made with melt extraction method.

and Tx of this fiber are a little higher than those of an amorphous ceramic $Al_{31}Gd_9O_{60}$ fiber [10]. The crystallization process can be considered as splitting into two stages similar to an amorphous ceramic $Al_{31}Gd_9O_{60}$ fiber [10]. We cannot identify a precipitated crystalline phase from the amorphous state after the first (1236 K) or the second exothermic peak (1371 K) from X-ray diffraction patterns showing only broad peaks.

3.2. Temperature dependence of tensile behavior of amorphous ceramic fibers

Fig. 4 shows temperature dependence of the tensile strength for the $Al_{32.4}Er_{7.6}O_{60}$ fiber. Although the fiber has a high tensile strength of about 900 MPa from room temperature to about 1100 K, the tensile strength falls precipitously above 1100 K and continues to drop with increasing testing temperatures. Fig. 5 is SEM image showing the external appearance in the fiber direction at 1273 K. When the temperature reaches 1273 K, the supercooled liquid state occurs and the tensile strength of the fiber drops to about 50 MPa (Fig. 4), and a jelly-like viscous flow deformation occurs (Fig. 5), indicating the occurrence of a superplastic deformation phenomenon, as in an amorphous ceramic $Al_{31}Gd_9O_{60}$ fiber [10]. At 573 K, the S-glass tensile strength is about 90% of the room temperature strength, dropping to about 50% at 773 K and to about 30% at 1023 K [8]. So the amorphous $Al_{32.4}Er_{7.6}O_{60}$ fiber is extremely superior, regarding the temperature dependence of tensile strength. In the supercooled liquid state, the fiber is compressed and ruptures as shown in Fig. 5, indicating an extremely sticky viscous fracture, rather than a brittle fracture. When the test temperature exceeds 1273 K, temperature distribution equivalent to the supercooled liquid range exists inside the electric furnace, so the stress-displacement curve shows the shape affected by a partial viscous deformation with slight improvement in tensile strength. Above 1373 K, the tensile strength drops gradually with increasing temperatures owing to the grain growth of constitutional phases. A ceramic

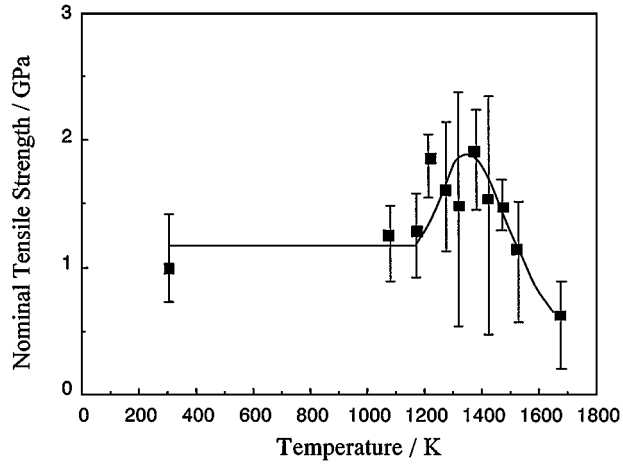

Figure 6 Heat treatment temperature versus tensile strength at room temperature of an amorphous $Al_{32.4}Er_{7.6}O_{60}$ continuous fiber made with melt extraction is heat treated at various temperatures for two hours in an air atmosphere.

Figure 5 SEM image showing the tip appearance of a tensile fractured fiber at 1273 K, of an amorphous $Al_{32.4}Er_{7.6}O_{60}$ continuous fiber made with melt extraction method.

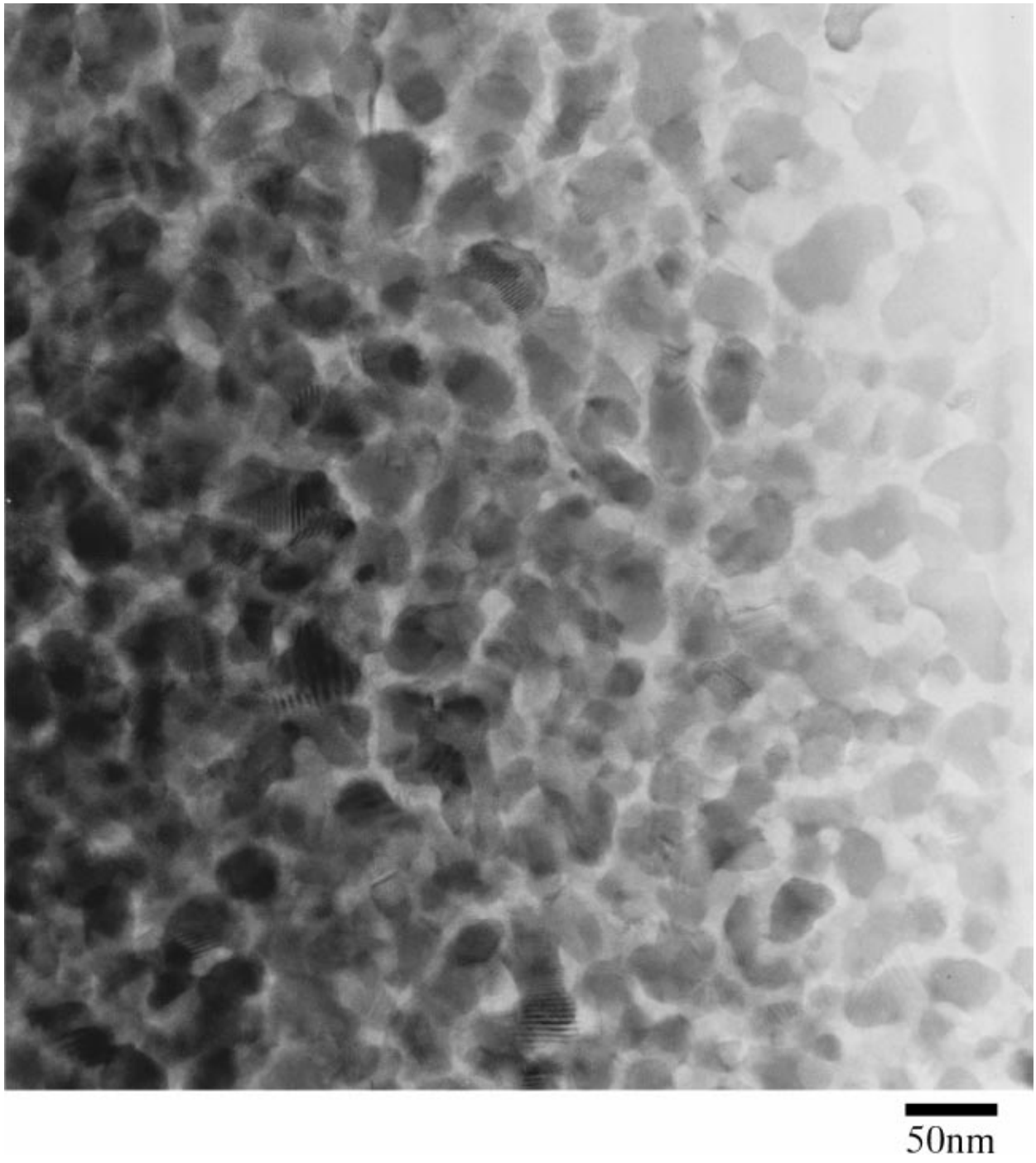

Figure 7 High resolution transmission electron micrograph of a $Er_3Al_5O_{12}$ nanocrystalline phase in an amorphous matrix after two hours of crystallization heat treatment at 1373 K in an air atmosphere of an amorphous $Al_{32.4}Er_{7.6}O_{60}$ continuous fiber made with melt extraction method.

crystalline fiber consisting of Al_2O_3 and $Er_3Al_5O_{12}$ phases in a uniform state can be obtained by heat treatment for 2 hours at 1473 K (from X-ray diffraction and SEM images).

3.3. Crystallization of amorphous ceramic fibers

Fig. 6 shows the relationship between heat treatment temperatures and tensile strength at room temperature, after 2 hours of heat treatment at each test temperature in an air atmosphere. The change in tensile strength depending on heat treatment temperatures can be divided into 3 regions. In region 1 (RT - 1173 K), the tensile strength is barely affected by the heat treatment temperature, so this region can be considered to be a region where the amorphous structure is stable. In region 2 (1173 K–1373 K), the tensile strength improves over that of region 1, reaching the maximum tensile strength of 1.9 GPa at 1373 K, or about 210% of the room temperature's tensile strength of an amorphous ceramic fiber. Fig. 7 is a high resolution transmission electron micrograph of the fiber microstructure after heat treatment was maintained for 2 hours at 1373 K in an air atmosphere, Fig. 8 is an X-ray diffraction pattern obtained from the same sample of Fig. 7. An $Er_3Al_5O_{12}$ phase with a size of around 20–40 nm exists homogeneously in an amorphous matrix (from Figs 7 and 8). In other words, a high-strength ceramic continuous fiber with a uniform nanocrystalline phase in the

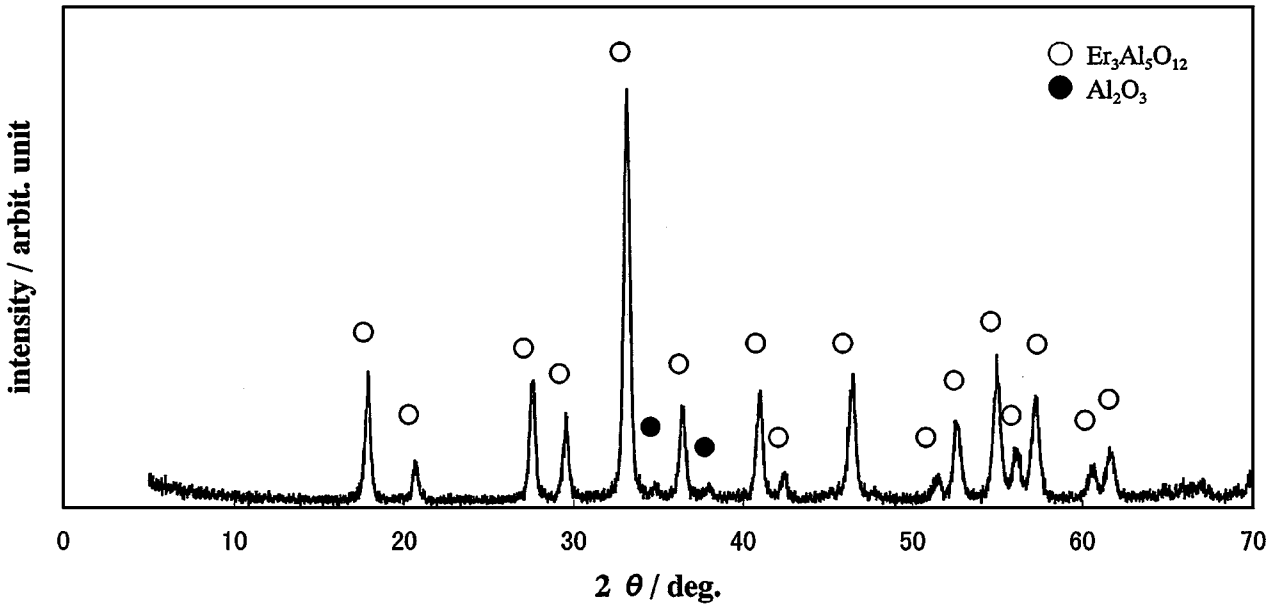

Figure 8 An X-ray diffraction pattern of a $Al_{32.4}Er_{7.6}O_{60}$ nanocrystallized fiber obtained by heat treatment at 1373 K for 2 hours in an air atmosphere.

amorphous matrix can be manufactured by controlling the crystallization from the amorphous state. The heat resistance, Young's modulus, hardness and other properties are therefore improved due to crystallization up to 1373 K. For instance, Young's modulus and Vickers hardness are changed from around 165 GPa (which can be estimated from the gradient of stress-strain curve) and around Hv 898 of an amorphous ceramic fiber to around 235 GPa and around Hv 1888 by the crystallization heat treatment at 1373 K for 2 hours.

In region 3 (above 1373 K), the tensile strength drops gradually with increasing temperatures owing to the grain growth of constitutional phases. A crystalline ceramic fiber consisting of Al_2O_3 and $Er_3Al_5O_{12}$ phases in a uniform state can be obtained by heat treatment for 2 hours at 1673 K (from X-ray diffraction and SEM images).

From X-ray diffraction results of the fiber after heat treatment for 2 hours at 1373 K and 1673 K, we can presume to precipitate a nanometersized $Er_3Al_5O_{12}$ crystalline phase at the first exothermic peak (1236 K) and a nanometersized Al_2O_3 crystalline at the second exothermic peak (1371 K) in Fig. 3.

4. Conclusions

The amorphous $Al_{32.4}Er_{7.6}O_{60}$ continuous fiber made with the melt extraction method differs from glass fibers and amorphous Al_2O_3 [8] or Al_2O_3-YAG fibers [9] in the following ways:

(1) Since glass fiber contains a large amount of SiO_2, CaO, and other elements, its strength starts to drop at a relatively low temperature. The amorphous $Al_{32.4}Er_{7.6}O_{60}$ continuous fiber shows no strength deterioration up to 1100 K, whereas the S-glass fiber strength at 1023 K is about 30% of the room temperature strength.

(2) Although the glass fiber's Young's modulus is about 70 GPa, that of the amorphous $Al_{32.4}Er_{7.6}O_{60}$ continuous fiber is about 165 GPa.

(3) A conventional amorphous Al_2O_3 fiber cannot exist in a supercooled liquid state, so it cannot undergo a jelly-like viscous flow deformation. We suppose that the appearance of the supercooled liquid state of this fiber is due to a stable amorphous structure and a combination of Al, Er and O elements containing a rare earth element, Er.

In ceramic fields, the ceramic superplastic process, which utilizes crystal grain rotation and grain boundary slipping or grain boundary liquid phases is recently being actively studied worldwide as potential secondary processing [11]. It has been reported that superplastic processing is possible at around 1723 K for an ionic crystal Y_2O_3-TZP (stabilized tetragornal ZrO_2 polycrystals) [12] and at around 1873 K for a covalent crystal Si_3N_4/SiC composite [13]. The amorphous $Al_{32.4}Er_{7.6}O_{60}$ continuous fiber can undergo large viscous flow deformation similar to glass and an amorphous ceramic $Al_{31}Gd_9O_{60}$ fiber at around 1273 K, so practical application as a ceramic that can be easily shaped at a relatively low temperature can be expected. Furthermore, a high-strength ceramic continuous fiber with an uniform nanocrystalline phase in an amorphous matrix can be obtained by the subsequent crystallization heat treatment.

Acknowledgment

This work was done under the support of NEDO. We thank N. Nakagawa of Ube Research Laboratory, UBE Industries, Ltd. and K. Shimizu of Japan Ultra-high Temperature Materials Research Institute for their assistance in experiments.

References

1. T. ISHIKAWA, Y. KOHTOKU, K. KUMAGAWA, T. YAMAMURA and T. NAGASAWA, *Nature* **391** (1998) 773.
2. M. TAKEDA *et al.*, *Ceram. Eng. Sci. Proc.* **12** (1991) 1007.

3. P. LAMICQ, G. A. BERNHART, M. M. DAUCHIER and J. G. MACE, *Am. Ceram. Soc. Bull.* **65** (1986) 336.
4. B. M. RABEEH, W. O. SCOBOYEJO, P. RAMASUNDARAM and T. S. SRIVATSAN, in "Processing Fabrication of Advanced Materials vol. 4," edited by T. S. Srivatsan and J. J. More (TMS, 1996) p. 609.
5. J. O. STRÖM-OLSEN, G. RUDKOWSKA, P. RUDKOWSKI, M. ALLAHVERDI and R. A. L. DREW, *Mater. Sci. Eng.* **A170**/**A180** (1994) 158.
6. M. ALLAHVERDI, R. L. DREW and J. O. STRÖM-OLSEN, *J. Mater. Sci.* **31** (1996) 1035.
7. F. T. WALLENBERGER, N. E. WESTON and S. A. DUNN, *SAMPE Quarterly* **21** (1990) 15.
8. *Idem., ibid*. **21** (1990) 30.
9. E. A. AGUILAR and A. A. L. DREW, *Journal of the European Ceramic Society* **20** (2000) 1091.
10. Y. WAKU, H. OHTSUBO and A. INOUE, *Mat. Res. Innovat.* **3** (2000) 185.
11. T. G. NEIH, J. WADSWORTH and F. WAKAI, *International Materials Reviews* **36** (1991) 146.
12. F. WAKAI, S. SAKAGUCHI and Y. MATSUNO, *Advanced Ceramic Materials* **1**(1) (1986) 259.
13. F. WAKAI, Y. KODAMA, S. SAKAGUCHI, N. MURAYAMA, K. IZEKI and K. NIIHARA, *Nature* **344** (1990) 421.

Received 5 July
and accepted 28 November 2000